Distinctive character of electronic and vibrational coherences in disordered molecular aggregates

ARTICLE *in* CHEMICAL PHYSICS LETTERS · MAY 2013

Impact Factor: 1.9 · DOI: 10.1016/j.cplett.2013.09.043 · Source: arXiv

4 AUTHORS, INCLUDING:

Vytautas Butkus
Vilnius University
25 PUBLICATIONS **234** CITATIONS
SEE PROFILE

Darius Abramavicius
Vilnius University
118 PUBLICATIONS **2,043** CITATIONS
SEE PROFILE

Distinctive character of electronic and vibrational coherences in disordered molecular aggregates

Vytautas Butkus,[1,2] Donatas Zigmantas,[3] Darius Abramavicius,[1,4] Leonas Valkunas,[1,2*]
[1] *Department of Theoretical Physics, Faculty of Physics, Vilnius University, Sauletekio 9-III, 10222 Vilnius, Lithuania*
[2] *Center for Physical Sciences and Technology, Gostauto 9, 01108 Vilnius, Lithuania*
[3] *Department of Chemical Physics, Lund University, P.O. Box 124, 22100 Lund, Sweden and*
[4] *State Key Laboratory of Supramolecular Complexes, Jilin University, 2699 Qianjin Street, Changchun 130012, PR China*

Coherent dynamics of coupled molecules are effectively characterized by the two-dimensional (2D) electronic coherent spectroscopy. Depending on the coupling between electronic and vibrational states, oscillating signals of purely electronic, purely vibrational or mixed character can be observed with the help of oscillation maps, constructed from the time-resolved 2D spectra. The amplitude of the beatings caused by the electronic coherence is heavily affected by the energetic disorder and consequently the electronic coherences are quickly dephased. Beatings with the vibrational character weakly depend on the disorder, assuring their long-time survival. We show that detailed modeling of 2D spectroscopy signals of molecular aggregates provides direct information on the origin of the coherent beatings.

I. INTRODUCTION

Dynamic properties of electronic excitations in artificial and biological molecular aggregates are determined by the intra- and intermolecular interactions. Due to resonant intermolecular interactions, electronic excitations of the aggregate form collective exciton states exhibiting coherent relationship between molecular excited states [1, 2]. Interactions with intramolecular vibrations reflect the specificity of molecular constituents of the aggregate and usually manifest themselves as vibrational sub-bands in electronic absorption or fluorescence spectra [3]. Depending on the relative strength of these interactions, the induced excitations in molecular aggregates may lead to a host of photoinduced dynamics: from coherent and incoherent energy migration to reorganization of the surrounding environment [4–6].

To resolve the details of the excitation evolution time-resolved spectroscopy techniques have been developed. Femtosecond coherent two-dimensional (2D) spectroscopy is one of the most versatile techniques [7, 8]. 2D spectroscopy has been already applied by considering the excitation dynamics in various molecular aggregates, e. g. photosynthetic pigment-protein complexes, polymers, tubular aggregates, quantum dots [9–14]. The inherent complexity of the 2D spectra was disclosed in all these cases. For instance, the long-lasting oscillatory features, initially attributed to electronic quantum coherences, have been resolved [11, 12, 15, 16]. Possible vibronic/vibrational origin of some of these beats has been proposed in a number of recent studies [17, 18]. Thus, it has been proved that coupling to multiple intramolecular vibrational modes is essential to determine the spectral properties of the most chromophore molecules resulting in complex behavior of the 2D spectra [17–21].

Since the role of the coherence is considered to be an important factor by defining the excitation dynamics in molecular aggregates the task of distinguishing electronic and vibrational character of coherences is essential and at the same time very challenging issue. To distinguish between the origins of the spectral oscillating behavior a molecular dimer (MD) as the simplest model of the vibronic molecular aggregate is considered. This work is a natural extension of our previous comparative study of coherent 2D spectra of vibrational monomer and electronically-coupled dimer (ED) [18]. Here we demonstrate that coherent oscillations of electronic and vibrational character are mixed due to intermolecular interactions. However, they exhibit distinct oscillation patterns and different behavior with respect to the energetic disorder.

II. MODEL

As usual for resonant spectroscopy applications let us assume that a constituent chromophore molecule of the aggregate is characterized by two levels corresponding to electronic ground and excited states and the electronic transitions are coupled to a single nuclear coordinate of high-frequency intramolecular vibrational mode with frequency ω_0. This coupling can be effectively represented in terms of the displaced harmonic oscillator model [2]. The electronic excitation results in the shift along the dimensionless coordinate q of the potential energy surface defined in the ground state as $V(q) = \omega_0 q^2/2$. Assuming the Heitler-London approximation [1] the Hamiltonian of

*Electronic address: leonas.valkunas@ff.vu.lt

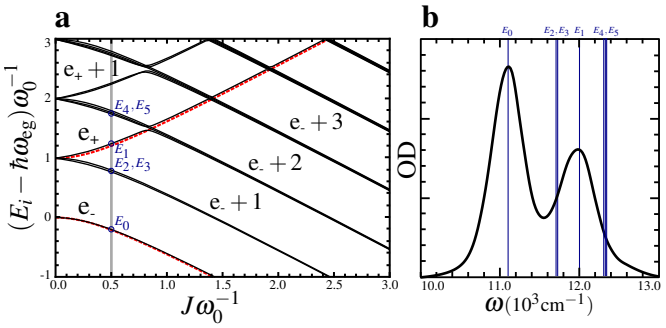

Figure 1: Dependence of the energies of the singly-excited states of the molecular dimer on the resonant coupling (a, black solid lines) in the case of small Huang-Rhys factors $s_1 = s_2 = 0.05$. A clear separation of electronic excited states (denoted as e_- and e_+, respectively) and vibronic states (denoted as $\mathrm{e}_\pm+m$, where m – the number of vibrational quanta) is observerd. The energies of a purely electronic dimer $E_{e_\pm}$ are represented by the red dashed lines. (b) The absorption spectrum of the molecular vibronic dimer with coupling $J = 0.5\omega_0$ is also shown, which corresponds to the energy states indicated by the vertical gray line in (a). Positions of the transitions contributing to the absorption spectrum are indicated by vertical lines.

the dimer is given by

$$\begin{aligned}\hat{H} = {} & T + [V(q_1) + V(q_2)]\,|\mathrm{g}\rangle\langle\mathrm{g}| \\ & + [\varepsilon_1 + V(q_1 - d_1) + V(q_2)]\,|\mathrm{e}_1\rangle\langle\mathrm{e}_1| \\ & + [\varepsilon_2 + V(q_1) + V(q_2 - d_2)]\,|\mathrm{e}_2\rangle\langle\mathrm{e}_2| \\ & + J\,[|\mathrm{e}_1\rangle\langle\mathrm{e}_2| + |\mathrm{e}_2\rangle\langle\mathrm{e}_1|] \\ & + [\varepsilon_1 + \varepsilon_2 + V(q_1 - d_1) + V(q_2 - d_2)]\,|\mathrm{f}\rangle\langle\mathrm{f}|, \end{aligned} \quad (1)$$

where $|\mathrm{g}\rangle$ is the electronic common ground state, $|\mathrm{e}_n\rangle$ corresponds to the electronic excited state of the n-th molecule of the dimer ($n = 1, 2$); $|\mathrm{f}\rangle$ is the doubly-excited state of the dimer, which corresponds to electronic excitations of both monomers. Term T represents the total kinetic energy of the vibrational harmonic oscillators coupled to both molecules, d_n is the displacement value of the vibrational potential in the electronically excited state, ε_n is the energy difference between the potential minima of $|\mathrm{g}\rangle$ and $|\mathrm{e}_n\rangle$ states of the n-th monomer, J is the resonance interaction. Since $V(q_n - d_n) - V(q_n) = \lambda_n - \omega_0 d_n q_n$ with $\lambda_n = \omega_0 d_n^2/2$ being the so-called reorganization energy, this difference in the potential energies determines the coupling of the electronic excitation to molecular vibrations. The latter is usually characterized by the dimensionless Huang-Rhys factor $s_n = d_n^2/2$.

In the case of no displacement ($s_1 = s_2 = 0$) the electronic excitations are not coupled to molecular vibrations and the electronic part of the Hamiltonian is easily diagonalized giving analytical expressions of the singly-excited state energies of the electronic dimer, $E_{e_\pm} = \omega_{\mathrm{eg}} \pm \Delta E_{\mathrm{ED}}$, where $\omega_{\mathrm{eg}} = \frac{1}{2}(\varepsilon_1 + \varepsilon_2)$ and $\Delta E_{\mathrm{ED}} = \frac{1}{2}\sqrt{(\varepsilon_2 - \varepsilon_1)^2 + 4J^2}$. Dependence of the exciton energies of the electronic dimer on the coupling is shown in Fig. 1a by the red dashed lines. The remaining vibrational Hamiltonian corresponds to the harmonic oscillator which can be easily quantized.

The ground-state Hamiltonian in Eq. (1) is diagonal by definition independently on the value of s_n and contains a ladder of vibrational states with energies spaced by ω_0. The singly-excited state block of the Hamiltonian is not diagonal in this basis and depends on the value of s_n. After numerical diagonalization, if a sufficient number of vibrational states ν_{vib} is taken into account, the excitation energies are found approximately at $E_{e_-} + \omega_0 m$ and $E_{e_+} + \omega_0 m$ ($m = 0, 1, \ldots$) and virtually constitute two ladders of equally-spaced states, denoted by $e_+ + m$ and $e_- + m$ in Fig. 1a. In the energy spectrum, the avoided crossing regions, where the electronic splitting matches vibrational quantum, emerge at particular values of the parameters when the most pronounced mixing of state character occurs [22]. For the larger Huang-Rhys factors ($s = 0.05$ is used in Fig. 1a) the deviation of the vibrational excitation energies from the harmonic ladder structure becomes significant, especially in the vicinity of the avoided crossing regions.

We denote the electronic ground state as the state where both molecules are in their ground states with arbitrary vibrational excitations, $|\mathrm{g}_i\mathrm{g}_j\rangle$. Index i here indicates the i-th vibrational excitation of the first molecule and j denotes the vibrational excitation of the second molecule. $|\mathrm{e}_1\rangle = |\mathrm{e}_i\mathrm{g}_j\rangle$ denotes the state of the first molecule being in the vibronic excited state maintaining the i-th vibration quantum and the second molecule being in the j-th vibrational ground state; analogously, $|\mathrm{e}_2\rangle = |\mathrm{g}_i\mathrm{e}_j\rangle$ corresponds to the state where the second molecule is vibronically excited. Doubly-excited electronic states $|\mathrm{f}\rangle = |\mathrm{e}_i\mathrm{e}_j\rangle$ are constructed in a similar way. Thus, the site basis of our model is complete with respect to vibronic states since one-particle vibronic states (such as $|\mathrm{e}_i\mathrm{g}_0\rangle$) and two-particle vibronic states ($|\mathrm{e}_i\mathrm{g}_j\rangle$, $j \neq 0$) are included. In terms of these definitions the vibronic set of eigenstates for the singly- and doubly-excited electronic states (state vectors $|u\rangle$ and $|v\rangle$, correspondingly) can be obtained by using the relevant transformations $|u\rangle = \sum_{ij}\left(\phi^{(1)}_{u,\mathrm{e}_i\mathrm{g}_j}|\mathrm{e}_i\mathrm{g}_j\rangle + \phi^{(2)}_{u,\mathrm{g}_i\mathrm{e}_j}|\mathrm{g}_i\mathrm{e}_j\rangle\right)$ and $|v\rangle = \sum_{ij}\Phi_{v,\mathrm{e}_i\mathrm{e}_j}|\mathrm{e}_i\mathrm{e}_j\rangle$. The corresponding transformation coefficients $\phi^{(n)}$ and Φ are acquired from the diagonalization of the singly-excited and doubly-excited blocks of the Hamiltonian (1) and provide us with the information about the eigenstate composition which allows the estimation of the amount of mixing between vibrational and electronic states.

The transition dipole moments between the ground and singly-excited states as well as between singly- and doubly-excited states in the vibronic eigenstate basis are then given by

$$\boldsymbol{\mu}_{u,\mathrm{g}_i\mathrm{g}_j} = \boldsymbol{\mu}_1\phi^{(1)}_{u,\mathrm{e}_i\mathrm{g}_j} + \boldsymbol{\mu}_2\phi^{(2)}_{u,\mathrm{g}_i\mathrm{e}_j} \quad (2)$$

and

$$\boldsymbol{\mu}_{vu} = \boldsymbol{\mu}_2 \sum_{ijlm} \phi^{(1)}_{u,\mathrm{e}_l\mathrm{g}_m} \Phi_{v,\mathrm{e}_i\mathrm{e}_j} + \boldsymbol{\mu}_1 \sum_{ijlm} \phi^{(2)}_{u,\mathrm{g}_l\mathrm{e}_m} \Phi_{v,\mathrm{e}_i\mathrm{e}_j}, \quad (3)$$

where $\boldsymbol{\mu}_1$ and $\boldsymbol{\mu}_2$ are the transition dipole moments of the monomers.

We will consider 2D signals of the molecular dimer, which are calculated using the perturbative system-response function theory in the vibronic eigenstate basis using the impulsive limit of the laser pulses, i.e. assuming that the laser pulse spectrum covers all frequencies. More information regarding the details of calculations can by found elsewhere [23, 24]. For the sake of simplicity, we assume the pure dephasing as the only mechanism responsible for the homogeneous lineshape formation. The energetic disorder (uncorrelated fluctuations of site energies ε_n) is considered to be responsible for the inhomogeneous broadening that is taken into account by averaging over ensemble (1000 realizations of independent simulations) with the Gaussian distribution with standard deviation σ_D of excitation energies for every molecule.

III. RESULTS

We consider the molecular dimer with Huang-Rhys factors equal for both monomers, $s \equiv s_1 = s_2$. We set vibrational frequency ω_0 as the reference parameter and choose the resonant coupling strength $J = -\omega_0/2$. We also choose that electronic site energies are separated by the same value as vibrational frequency, $\varepsilon_2 - \varepsilon_1 = \omega_0$. As values typical for aggregates, we consider $\omega_0 = 600\,\mathrm{cm}^{-1}$ and $s = 0.05$, thus resulting in $\Delta E_\mathrm{MD} \approx 867\,\mathrm{cm}^{-1}$, which is approximately equal to the excitonic splitting of the electronic dimer ΔE_ED. Hence, the excitonic splitting is off-resonant with respect to the vibronic resonance (compare e_+, e_- and $\mathrm{e}_- + 1$ levels Fig. 1a). We assume that the strengths of the transition dipole moments of the monomers are equal and constitute the inter-dipole angle $\varphi = \frac{2\pi}{5}$. The dephasing rate determining the homogeneous linewidth is set to $\gamma = \omega_0/6$ and central absorption frequency is chosen $\omega_\mathrm{eg} = 11500\,\mathrm{cm}^{-1}$. For numerical calculations we choose $\nu_\mathrm{vib} = 8$; calculations with more vibrational states show no evident changes in any simulated spectroscopic signals for the used set of parameters. The deviation from a harmonic ladder of vibronic sates appears, but is insignificant for the model considered here, as the singly-excited state energy departure from the ideal harmonic progression is less than 5% and the chosen parameters ensure that we are away from the avoided-crossing regions (see Fig. 1a).

The electronic interaction with the high-frequency vibrational mode is almost indistinguishable in the absorption spectrum for the chosen small value of the Huang-Rhys factor as the only evidence of vibronic content is a sole weak shoulder in absorption at $\sim 12600\,\mathrm{cm}^{-1}$ (Fig. 1b). For the larger Huang-Rhys factor the stronger vibrational progression would evidently appear in the spectrum. However, consideration of such an aggregate instead would not change conclusions of the further discussion appreciably.

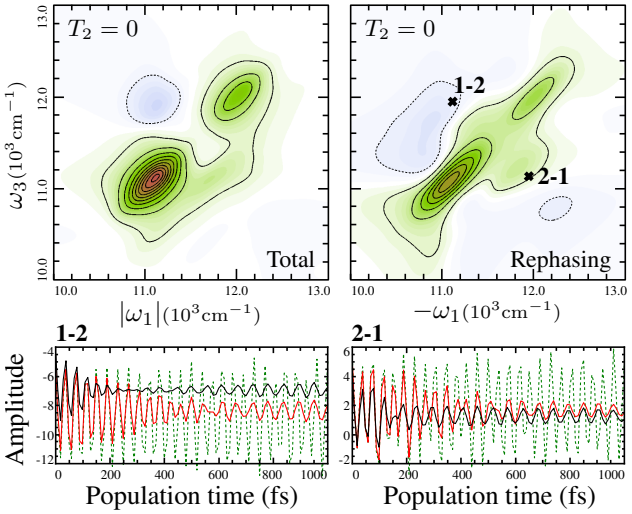

Figure 2: The total (a sum of rephasing and non-rephasing) and only rephasing 2D spectra of the molecular dimer at the population time $T_2 = 0$, with Gaussian disorder $\sigma_\mathrm{D} = 200\ \mathrm{cm}^{-1}$ (upper panels). Solid (dashed) contour lines for positive (negative) signals are drawn in 10% intervals. Time dependences of the amplitudes of the upper (1-2) and lower (2-1) cross-peaks of the rephasing signal are shown in the lower panels (left and right, respectively). Green – no disorder, red – $\sigma_\mathrm{D} = 20\,\mathrm{cm}^{-1}$, black – $\sigma_\mathrm{D} = 50\,\mathrm{cm}^{-1}$.

Transition amplitudes $\mu_{u,\mathrm{g}_i\mathrm{g}_j}$ between the ground state manifold of the vibrational states and the manifold corresponding to the singly-excited states signify possible interaction configurations. The "vibronic content" in a specific electronic transition can be quantified by the transformation coefficients combined as $\chi_u \equiv \left(\phi^{(1)}_{u,\mathrm{g}_0\mathrm{g}_0}\right)^2 + \left(\phi^{(2)}_{u,\mathrm{g}_0\mathrm{g}_0}\right)^2$. The maximum value of this quantity ($\chi_u = 1$) indicates the pure electronic character of the state, while $\chi_u = 0$ reflects that the corresponding transition is vibronic. Transitions originating from the zero-vibrational state, i. e. $|\mathrm{g}_0\mathrm{g}_0\rangle$ are described in Table I. The two most significant transitions correspond to electronic-only transitions with $\chi \geq 0.9$, while the other transitions are of dominant vibrational character ($\chi < 0.1$).

The real parts of rephasing and total 2D spectra contain three positive features: two diagonal peaks and a clearly distinguishable cross-peak (2-1) below the diagonal reflecting the coherent resonance coupling between the molecules (Fig. 2). The higher cross-peak (1-2) is less visible due to the overlap with the excited state absorption (ESA) contribution. Apparent simple structure of the spectra the complicated pattern of various overlapping contributions. They can be sorted into: i) *stationary contributions*, denoting the excitation pathways, where the aggregate is in a population state during delay time T_2; ii) *oscillating contributions*, reflecting the co-

u	$E_u - E_0$, cm^{-1}	μ_{u,g_0g_0}	χ_u	φ_u, deg	States in site basis					
					$\|e_0g_0\rangle$	$\|g_0e_0\rangle$	$\|e_1g_0\rangle$	$\|g_0e_1\rangle$	$\|e_0g_1\rangle$	$\|g_1e_0\rangle$
0	0	1.08	0.96	19.0	**0.82**	**0.14**	0.03	0.00	0.00	0.00
1	867	0.84	0.90	-81.8	**0.15**	**0.76**	0.02	0.01	0.05	0.01
2	581	0.26	0.06	69.3	0.00	0.06	**0.37**	0.09	**0.37**	0.06
3	600	0.17	0.02	19.0	0.02	0.00	**0.38**	0.07	**0.41**	0.07
4	1467	0.13	0.02	-81.3	0.00	0.02	0.09	**0.36**	0.06	**0.36**
5	1480	0.11	0.01	69.8	0.00	0.01	0.08	**0.33**	0.08	**0.36**

Table I: Mixed character of the lowest vibronic eigenstates of the molecular dimer with the Huang-Rhys factor $s = 0.05$. Value of $\chi_u = 1$ signifies a completely electronic character of the exciton state, while $\chi_u = 0$ corresponds to the vibrational character. φ_u denotes the angle of corresponding transition dipole vector with respect to the electronic transition dipole of the first monomer. $E_u - E_0$ correponds to the energy gap between vibronic sates and μ_{u,g_0g_0}– to the transition dipole moment.

herent electronic or vibronic excitation dynamics in the excited state or vibrational dynamics in the ground state. The multitude of the later ones in case of the molecular dimer system is illustrated in Fig. 3a. Temporal dynamics of oscillating contributions can be represented by the time dependent traces of certain spectral regions. Such traces of upper (1-2) and lower (2-1) cross-peaks of the rephasing signal are presented in the lower panel of Fig. 2. The oscillations can also be characterized by studying the so-called oscillation Fourier maps which are constructed by applying the Fourier transform to the real part of the rephasing spectrum $S_{\rm R}(\omega_3, T_2, \omega_1)$ with respect to the delay time T_2 [25, 26],

$$A(\omega_3, \omega_2, \omega_1) = \int_0^\infty {\rm d}T_2 e^{{\rm i}\omega_2 T_2} {\rm Re} S_{\rm R}(\omega_3, T_2, \omega_1). \qquad (4)$$

This allows us to directly identify the phase and amplitude of oscillations in the different spectral regions. Such oscillation maps of the 2D spectra at frequencies corresponding to $\omega_2 = \omega_0$ and $\omega_2 = \Delta E_{\rm MD}$ are presented in figures 3b and 3c in case of no disorder ($\sigma_{\rm D} = 0$) and substantial disorder ($\sigma_{\rm D} = 200\,{\rm cm}^{-1}$), respectively. The oscillation map at $\omega_2 = \Delta E_{\rm MD}$ involves two states with the most pronounced electronic character (see Table I) and is the same as the purely electronic coherence map of an excitonic dimer [18], i.e. oscillations in the rephasing part appear only in the cross-peaks. As we find in the disordered system ($\sigma_{\rm D} = 200\,{\rm cm}^{-1}$) the oscillating patterns are completely dominated by the vibrational frequency ω_0, while the oscillations with the electronic gap frequency $\Delta E_{\rm MD}$ are at least 20 times weaker and, thus, their contribution is negligible. The oscillation map of the disordered vibronic dimer is highly asymmetric, which is mostly due to the ground state bleaching (GSB) contribution (Fig. 3a).

It is known that the phase of spectral oscillations of the electronic-only systems is 0 at the maxima of the peaks and changes continuously when going away from the peak (rises in direction outwards the diagonal). For the monomer coupled to a single mode of high-frequency vibration, the phase of either 0 or π can be obtained depending on the coupling strength [27]. However, in congested spectra any phase relationships can be obtained if the spectral overlap is substantial. Especially for the mixed system, when both resonance coupling and vibronic interactions are taken into account. For example, it can be seen in the oscillation map in Fig. 3c that at the center of the lower diagonal peak the phase is detuned by $\pi/3$ from the value of π, which would be expected for an isolated oscillating peak [19, 27].

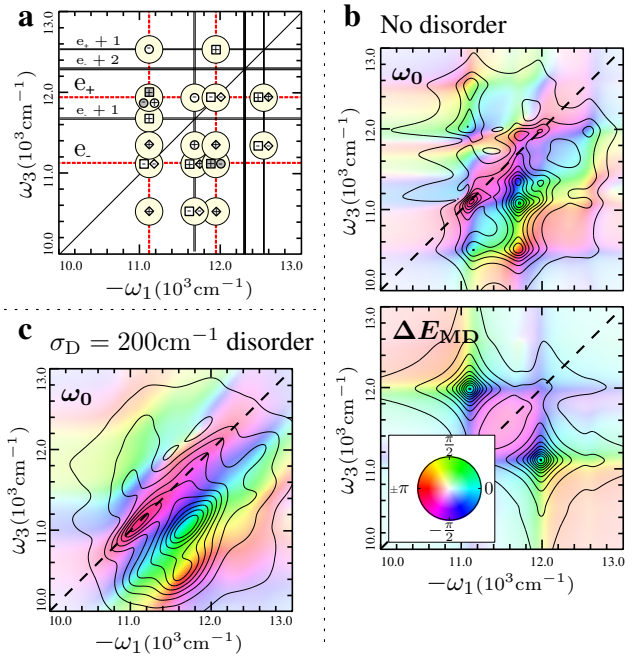

Figure 3: (a) Arrangement of the the most significant (90% of the total amplitude) oscillatory contributions (diamonds denote GSB, squares – SE and circles – ESA) in the 2D spectrum of the molecular dimer. The oscillations are at vibrational frequency ω_0 (open symbols) or electronic frequency $\Delta E_{\rm MD}$ (full gray symbols) and the plus/minus sign at each peak denotes the phase of the oscillation. (b) The Fourier maps are represented by the amplitude and phase of oscillations as contour lines and peak color, respectively, at frequencies ω_0 and $\Delta E_{\rm MD}$ when $\sigma_{\rm D} = 0$. (c) The oscillation map at frequency ω_0 when $\sigma_{\rm D} = 200\,{\rm cm}^{-1}$. The map at $\Delta E_{\rm MD}$ frequency is not shown since it has a negligible amplitude.

IV. DISCUSSION

The parameter set used in calculations describes a very general electronic-vibronic system. The chosen values $|J| = \omega_0/2$ do not correspond to any special case since the monomer energies remain different, $\varepsilon_2 \neq \varepsilon_1$. The chosen absolute values of parameters are typical for many molecular aggregates of interest, including the photosynthetic pigment-protein complexes. Similar parameters have already been used by investigating the vibronic transition dipole moment borrowing and coherence enhancement effects in molecular dimer systems [22, 28]. The introduced model captures both limiting cases of purely vibrational and purely electronic model systems that are usually considered separately. Indeed, by assuming either the Huang-Rhys factors or the resonance interaction to be zero both limiting cases can be obtained. Two prominent frequencies are present in the simulated oscillatory dynamics of the 2D spectrum of the vibronic molecular system. Evidently, one frequency corresponds to the electronic energy gap ΔE_{MD}, while the other is equal to the vibrational frequency ω_0. These coherences are between the states of mixed electronic-only and electronic-vibronic character, respectively (Table I). It is noteworthy to mention, that a very similar amount of mixing is obtained using even simpler description with only one-particle vibronic states and $\nu_{\mathrm{vib}} = 2$ included [22]. The mixed character might indirectly appear more significant if the diagonal disorder is comparable to the gap between states of different character. Then, the states of different character become overlapping leading to more mixing [28]. However, the distribution of the transition frequencies not the amount of mixing of particular state defines the oscillations. Thus, beatings with rather electronic and rather vibrational character still result in distinct oscillation maps and therefore the origin of the oscillation can be identified.

Strength of oscillations strongly depends on system inhomogeneity. From simulations, this can clearly be seen in the lower panel of Fig. 2, where time dependences of the peak value for different values of the Gaussian disorder ($\sigma_{\mathrm{D}} = 0$, 20 and $50\,\mathrm{cm}^{-1}$) are presented. The initial intensive oscillations with the ΔE_{MD} frequency decay rapidly when the disorder is increased and the only dynamics observed at longer delay times correspond to the ω_0 beats. Strengths of the oscillations at different frequencies are represented by the corresponding values of the amplitude in the oscillation maps. Therefore, the value of the amplitude maximum of the oscillation map is used to evaluate the strength of the corresponding oscillation. The amplitude of electronic oscillations decays sharply with the disorder, while dependence of the amplitude of vibronic/vibrational coherences is much more flat (the amplitudes for the stimulated emission (SE), excited state absorption (ESA) and ground state bleaching (GSB) contributions are presented in Fig. 4). When disorder is absent, signatures of electronic coherences mostly coming from the SE contribution are at least 5 times larger than those of vibrational character, while for $\sigma_{\mathrm{D}} > 200\,\mathrm{cm}^{-1}$ the amplitude of electronic coherences is negligible (the corresponding oscillation map for $\sigma_{\mathrm{D}} = 200\,\mathrm{cm}^{-1}$ cannot be resolved).

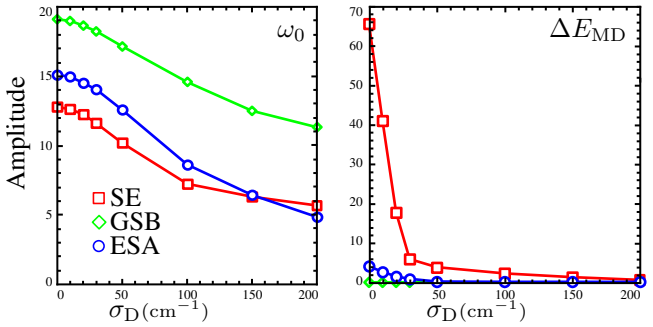

Figure 4: Maximal amplitude of the oscillation, taken from the oscillation maps as a function of disorder for GSB (diamonds), SE (squares) and ESA (circles) contributions at different beating frequencies (ω_0 and ΔE_{MD}).

Separation of coherences of electronic and vibrational character is very significant as our results demonstrate that besides vibrational beats the electronic beats could be in principle observed and distinguished for the weakly disordered systems. However, the electronic beats rapidly decay in time in a Gaussian fashion (for the Gaussian disorder) as σ_{D}^{-1}. Whereas vibrational beats will prevail for longer times.

Note that in the Hamiltonian used (Eq. 1) no transformation of canonical variables into symmetric and antisymmetric components is performed that would allow us to decouple the Schrdinger equations of the excited and ground states. Therefore, presented model contains states which are not separated to diabatic or adiabatic ones as has been done in the theoretical work of Jonas and coworkers addressing coherences in FMO [19]. Also, since we show the separation of beats of electronic and vibrational character for arbitrary system parameters, the resonant condition of the mixed character coherences (for example, when electronic energy gap or the chromophore energy difference is equal to the vibrational frequency) is just a special case of our model. It supports the assumptions about coherences in FMO where such resonant conditions are met – electronic coherences at initial times could be of the same order as those of the vibronic origin due to disorder of approximately 25 cm^{-1}; electronic beats will decay in a short time (~200 fs) while vibrational beats would persist over the long time. For higly disordered and uncorrelated systems electronic coherences are not likely to be significant at all and the observed coherent dynamics are due to the ground-state vibrations.

It is also important to consider transition dipole moment orientations φ_u listed in Table I. The orientations of the transitions to the "mixed" states are different for each state and are also different from the transition dipole moments of monomer transitions. This im-

plies that coherences involving arbitrary states (of electronic or vibrational character) might survive the measurements with polarization schemes, devised to suppress all but electronic coherence signals [15, 29]. On the other hand, these polarization schemes can then be used to distinguish between purely vibrational (localized on one molecule) and mixed origin coherences.

Results presented here are related to the assumption that the vibrational frequencies are not affected by inhomogeneities, which induce the disorder of electronic transition energy. This is often the case as vibrational resonances are less sensitive to the electrostatic configuration of the environment than the delocalized electronic wavefunctions. Vibrational coherences, hence, decay on a timescale of vibrational dephasing, which usually is in the order of a picosecond. It should be also noted that when vibrational frequency ω_0 matches the electronic energy gap ΔE_{MD}, the quantum mechanical mixing complicates the whole picture. Then damping of the resulting electronic-vibrational coherence will define the decay timescale of the oscillations in the spectra.

V. CONCLUSIONS

Coherent dynamics of coupled molecules can be effectively sorted out by the modeling of 2D spectra. Coupling between the multitude of vibrational states on different molecules results in a manifold of mixed states. When vibrational frequency and the electronic energy gap are off resonance this manifold constitutes two ladders of equally-spaced and well-resolved states. Two types of beats having either electronic or vibrational character can then be distinguished by the use of oscillation maps, constructed from the sequences of time-resolved 2D spectra.

Inhomogeneous disorder effects the coherences of different state character differently. The amplitude of the electronic character beatings, caused by the coherences in excited states, is dramatically reduced by the disorder and consequently electronic coherences are quickly dephased. Vibrational character beatings stem from the ground and excited state contributions and depend weakly on the disorder, assuring their long-time survival.

Acknowledgments

This research was partially funded by the European Social Fund under the Global grant measure. V. B. acknowledges support by project "Promotion of Student Scientific Activities" (VP1-3.1-MM-01-V-02-003) from the Research Council of Lithuania. D. Z was supported by the Swedish Research Council.

[1] M. Pope and C. E. Swenberg. *Electronic processes in organic crystals and polymers*. Oxford University Press, New York/Oxford, 2 edition, 1999.

[2] H. van Amerongen, L. Valkunas, and R. van Grondelle. *Photosynthetic Excitons*. World Scientific Co., Singapore, 2000.

[3] Robert L. Fulton and Martin Gouterman. Vibronic coupling. II. Spectra of dimers. *J. Chem. Phys.*, 41(8):2280–2286, 1964.

[4] Jin Sun, Bin Luo, and Yang Zhao. Dynamics of a one-dimensional Holstein polaron with the Davydov ansätze. *Phys. Rev. B*, 82:014305, Jul 2010.

[5] R-X. Xu, P. Cui, X-Q. Li, Y. Mo, and Y-J. Yan. Exact quantum master equation via the calculus on path integrals. *J. Chem. Phys.*, 122:041103, 2005.

[6] Andrius Gelzinis, Darius Abramavicius, and Leonas Valkunas. Non-markovian effects in time-resolved fluorescence spectrum of molecular aggregates: Tracing polaron formation. *Phys. Rev. B*, 84:245430, Dec 2011.

[7] S. Mukamel. Multidimensional femtosecond correlation spectroscopies of electronic and vibrational excitations. *Annu. Rev. Phys. Chem.*, 51:691–729, 2000.

[8] D. M. Jonas. Two-dimensional femtosecond spectroscopy. *Annu. Rev. Phys. Chem.*, 54:425–463, 2003.

[9] T. Brixner, J. Stenger, H. M. Vaswani, M. Cho, R. E. Blankenship, and G. R. Fleming. Two-dimensional spectroscopy of electronic couplings in photosynthesis. *Nature*, 434(7033):625–628, 2005.

[10] D. Zigmantas, E. L. Read, T. Mančal, T. Brixner, A. T. Gardiner, R. J. Cogdell, and G. R. Fleming. Two-dimensional electronic spectroscopy of the B800-B820 light-harvesting complex. *Proc. Natl. Acad. Sci. USA*, 103(34):12672–12677, 2006.

[11] G. S. Engel, T. R. Calhoun, E. L. Read, T. K. Ahn, T. Mančal, Y. C. Cheng, R. E. Blankenship, and G. R. Fleming. Evidence for wavelike energy transfer through quantum coherence in photosynthetic systems. *Nature*, 446:782, 2007.

[12] E. Collini and G. D. Scholes. Coherent intrachain energy migration in a conjugated polymer at room temperature. *Science*, 323(5912):369–373, 2009.

[13] Jaroslaw Sperling, Alexandra Nemeth, Jürgen Hauer, Darius Abramavicius, Shaul Mukamel, Harald F. Kauffmann, and Franz Milota. Excitons and disorder in molecular nanotubes: A 2d electronic spectroscopy study and first comparison to a microscopic model. *J. Phys. Chem. A*, 114(32):8179–8189, 2010.

[14] Daniel B. Turner, Krystyna E. Wilk, Paul M. G. Curmi, and Gregory D. Scholes. Comparison of electronic and vibrational coherence measured by two-dimensional electronic spectroscopy. *J. Phys. Chem. Lett.*, 2(15):1904–1911, 2011.

[15] Sebastian Westenhoff, David Paleček, Petra Edlund, Philip Smith, and Donatas Zigmantas. Coherent picosecond exciton dynamics in a photosynthetic reaction center. *J. Am. Chem. Soc.*, 134(40):16484–16487, 2012.

[16] Gitt Panitchayangkoon, Dmitri V. Voronine, Darius Abramavicius, Justin R. Caram, Nicholas H. C. Lewis, Shaul Mukamel, and Gregory S. Engel. Direct evidence of quantum transport in photosynthetic light-harvesting

complexes. *Proc. Natl. Acad. Sci. USA*, 108(52):20908–20912, 2011.

[17] Niklas Christensson, Harald F. Kauffmann, Tõnu Pullerits, and Tomàš Mančal. Origin of long-lived coherences in light-harvesting complexes. *J. Phys. Chem. B*, 116(25):7449–7454, 2012.

[18] V. Butkus, D. Zigmantas, L. Valkunas, and D. Abramavicius. Vibrational vs. electronic coherences in 2D spectrum of molecular systems. *Chem. Phys. Lett.*, 545:40–43, 2012.

[19] Vivek Tiwari, William K. Peters, and David M. Jonas. Electronic resonance with anticorrelated pigment vibrations drives photosynthetic energy transfer outside the adiabatic framework. *Proc. Natl. Acad. Sci. USA*, 110(4):1203–1208, 2013.

[20] Tomáš Mančal, Niklas Christensson, Vladimír Lukeš, Franz Milota, Oliver Bixner, Harald F. Kauffmann, and Jürgen Hauer. System-dependent signatures of electronic and vibrational coherences in electronic two-dimensional spectra. *J. Phys. Chem. Lett.*, 3(11):1497–1502, 2012.

[21] A. W. Chin, J. Prior, R. Rosenbach, F. Caycedo-Soler, S. F. Huelga, and M. B. Plenio. The role of non-equilibrium vibrational structures in electronic coherence and recoherence in pigment-protein complexes. *Nature Phys.*, 9(2):113–118, February 2013.

[22] Sergey Polyutov, Oliver Kühn, and Tõnu Pullerits. Exciton-vibrational coupling in molecular aggregates: Electronic versus vibronic dimer. *Chem. Phys.*, 394(1):21–28, 2012.

[23] D. Abramavicius, V. Butkus, J. Bujokas, and L. Valkunas. Manipulation of two-dimensional spectra of excitonically coupled molecules by narrow-bandwidth laser pulses. *Chem. Phys.*, 372(1-3):22–32, 2010.

[24] D. Abramavicius, L. Valkunas, and S. Mukamel. Transport and correlated fluctuations in the nonlinear optical response of excitons. *Europhys. Lett.*, 80(1):17005, 2007.

[25] Daniel B Turner, Rayomond Dinshaw, Kyung-Koo Lee, Michael Belsley, Krystyna E Wilk, Paul MG Curmi, and Gregory Scholes. Quantitative investigations of quantum coherence for a light-harvesting protein at conditions simulating photosynthesis. *Phys. Chem. Chem. Phys.*, 14:4857–4874, 2012.

[26] T. R. Calhoun, N. S. Ginsberg, G. S. Schlau-Cohen, Y-C. Cheng, M. Ballottari, R. Bassi, and G. R. Fleming. Quantum coherence enabled determination of the energy landscape in light-harvesting complex II. *J. Phys. Chem. B*, 113:16291–16295, 2009.

[27] Vytautas Butkus, Leonas Valkunas, and Darius Abramavicius. Molecular vibrations-induced quantum beats in two-dimensional electronic spectroscopy. *J. Chem. Phys.*, 137(4):044513, 2012.

[28] Aurélia Chenu, Niklas Christensson, Harald F Kauffmann, and Tomáš Mančal. Enhancement of vibronic and ground-state vibrational coherences in 2d spectra of photosynthetic complexes. *Sci. Rep.*, 3:2029, 2013.

[29] Gabriela S. Schlau-Cohen, Tessa R. Calhoun, Naomi S. Ginsberg, Elizabeth L. Read, Matteo Ballottari, Roberto Bassi, Rienk van Grondelle, and Graham R. Fleming. Pathways of energy flow in lhcii from two-dimensional electronic spectroscopy. *J. Phys. Chem. B*, 113(46):15352–15363, 2009.